QUANTIFYING THE IMPACT OF THE MC-CDMA PHYSICAL LAYER ALGORITHMS ON THE DOWNLINK CAPACITY IN A MULTI-CELLULAR ENVIRONMENT

Abdel-Majid Mourad[1], Arnaud Guéguen[1], and Ramesh Pyndiah[2]
[1]*Mitsubishi Electric ITE-TCL, Telecommunications Research Laboratory, Rennes, France;*
[2]*Ecole Nationale Supérieure des Télécommunications de Bretagne, Brest, France*

Abstract: In this paper, we present an evaluation methodology for quantifying the impact of the MC-CDMA physical layer algorithms on the system capacity in the downlink of a multi-cellular environment. The methodology consists of a qualitative evaluation through a novel capacity indicator at the link level and a quantitative evaluation through a semi-analytical statistical approach at the system level. The qualitative and quantitative evaluations are complementary and lead to similar and consistent conclusions. They constitute an efficient tool that can be used for optimizing the MC-CDMA physical layer algorithms and identifying the most suitable configurations for a given environment.

Key words: MC-CDMA, Outage capacity, Multi-cellular environment, Downlink.

1. INTRODUCTION

A complete and realistic evaluation of the performance of a cellular system requires joint consideration of both microscopic and macroscopic aspects, from the microscopic level of binary information transmission to the macroscopic level of network control mechanisms. A typical cellular system usually includes several cells and a large number of mobile users, and therefore a combined approach where the microscopic and macroscopic aspects are modeled into one single simulator would lead to very complex simulations of large time consumption. Thus, for obvious complexity and feasibility reasons, the combined approach is usually discarded in practice and another splitting approach is used instead. The splitting approach carries out the performance evaluation in two simulation phases: at *link level* and at *system level*, with suitable interfacing between the two levels [1][2].

A *link level simulator* typically includes a transmitter, a multi-path fading channel, and a receiver. It operates with a microscopic time resolution equal to the sampling period so that the physical layer algorithms and multi-path channel can be modeled exhaustively. The main concern here is to investigate the impact of the physical layer algorithms on the quality of the binary information transmitted through the multi-path fading channel between the transmitter and receiver. This is with the aim of accounting for the effectiveness of the physical layer algorithms and their robustness to multi-path channel impairments. The transmission quality of the binary information is measured in terms of the average bit (BER) and frame (FER) error rates, which are usually determined from link level simulations spanning a large number of frames experiencing independent fading.

The *system level simulator* typically includes several base stations and all the mobiles that are connected to these base stations. The main interests here are to evaluate the cellular capacity and coverage of the system and to develop proper *Radio Resource Management* (RRM) algorithms for appropriate sharing of the system resources among the mobile users. The system level simulations are more or less complex depending on how accurate and how realistic the models represented are. Two approaches of system level simulations are usually used [1][2]: the *static* and *dynamic* approaches. The static approach requires low computational costs and does not have time dependency. It has been extensively used in the literature for preliminary system level studies as it can easily and efficiently provide meaningful statistical capacity and coverage estimates [2]. The dynamic approach is a much more sophisticated time-based approach, which is much more accurate and realistic than the static approach, but at the expense of much higher complexity [2]. In this paper, the static approach is adopted instead of the dynamic approach as our objective is to investigate only the capacity benefits of the MC-CDMA physical layer algorithms in the downlink of a cellular system.

Because of the separation between link and system level simulations, a suitable interface between the two levels needs therefore to be defined. The target of the interface is to enable the system level simulators to predict easily and accurately the actual transmission quality of the different links in the system. This is because the transmission quality of the different links cannot be measured online within the system level simulations. Usual procedures to interface link and system levels are to use a set of *Look-Up Tables* (LUTs) mapping the BER and FER transmission quality measures to an adequate *Signal to Interference plus Noise Ratio* (SINR)-based measure that can easily be calculated at the system level. Different LUTs generally need to be produced for different operating conditions, and different levels of accuracy can be targeted depending on the particular study carried out at the system level [3].

In this study, since we only focus on the performance evaluation of the physical layer algorithms through static system level simulations, we consider the conventional transmission quality measure of the physical layer, i.e. FER averaged over a large number of frames experiencing independent fading, in order to set the requirements for link satisfaction at the system level. The average FER measure is simply mapped to the *local mean SINR* measure through the so-called *multi-frame oriented link to system interface* [6]. The local mean SINR is the ratio between the average signal power and average interference plus noise power at the output of the detection module. The multi-frame oriented link to system interface considered here is simple and provides a degree of accuracy that is acceptable for the objective targeted in this study.

The rest of this paper is organized as follows. Section 2 presents briefly the system model and then Section 3 presents the evaluation methodology for quantifying the impact of the MC-CDMA physical layer algorithms on the downlink multi-cellular capacity. Numerical results are then presented in Section 4 and conclusions are finally drawn in Section 5.

2. SYSTEM MODEL

We consider the MC-CDMA physical layer in the downlink of an hexagonal regular macro-cellular system [6]. The system is made up of one central cell surrounded by N tiers of neighboring cells. The number of cells in the system is therefore equal to:

$$Q = 1 + 3N(N+1) \tag{1}$$

Each cell has a centrally located BS fit with an omni-directional antenna. Each BS has at its disposal a maximum number of M spreading codes, and its total output power is limited by P_{max}. For the sake of simplicity and in order to avoid the border effects [4], the results are collected only from the central cell although the whole system is simulated, and the Q-1 neighboring BS are assumed to transmit at the same fixed power $P_o \leq P_{max}$. The users are assumed uniformly distributed within the disk delimiting the hexagonal cells (see Fig. 1). The connectivity between users and BSs follows the minimum path loss criterion, i.e. a user is connected to the BS to which the path loss is minimum. A user is connected only to one BS, i.e. there is no handover, and all users are assumed to have the same physical layer configuration.

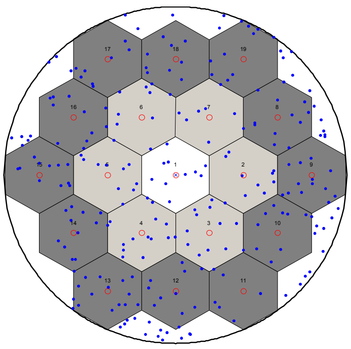

Figure 1. Cellular layout with $N = 2$ tiers and 250 users uniformly distributed within the disk delimiting the 19 hexagonal cells.

3. EVALUATION METHODOLOGY

Let us consider the problem of satisfying the target FER requirements of the users connected to the central BS (BS_1). Thanks to the direct mapping between the local mean SINR and average FER [6], the target FER can then be replaced by a target SINR. As discussed in [6], the target SINR value is specific to the given physical layer configuration and channel model. The problem of satisfying the SINR requirements under the constraint of limited BS power can then be formulated as:

$$SINR_k = \lambda_\phi, \quad \forall k = 1 \ldots K \le M, \quad p_k > 0, \quad P_c = \sum_{k=1}^{K} p_k \le P_{\max} \tag{2}$$

where λ_ϕ denotes the target SINR that is specific to the physical layer configuration ϕ, K is the cell load of BS_1, P_c is BS_1 output power, and p_k is the power BS_1 should allocate to its k-th user in order to satisfy the SINR requirements. At last, $SINR_k$ denotes the local mean SINR at the output of the single user detection (SUD) module of the k-th user connected to BS_1 and it is given by [6]:

$$SINR_k = \frac{p_k g_{1k}}{g_{1k} \sum_{j=1, j \ne k}^{K} p_j \alpha_{kj} + \beta_k \left(\frac{1}{SF} \sum_{q=2}^{Q} P_o g_{qk} + P_n \right)} \tag{3}$$

where g_{qk} stands for the path loss between BS_q and user k of BS_1. The quantities $\{\alpha_{kj}\}$ and β_k are respectively the mutual intra-cell interference and inter-cell interference plus noise factors at the output of the SUD module. These factors are derived analytically in [6] from the equalized channel coefficients correlation and family of spreading codes. At last, SF is the spreading factor and P_n is the thermal noise power.

Making use of (3), (2) can be rewritten as the following power allocation problem for BS_1:

$$\mathbf{p} = \lambda_\phi \left(\mathbf{A}\mathbf{p} + \mathbf{f} P_o + \mathbf{b} P_n \right), \quad \mathbf{p} > \mathbf{0}, \quad P_c = \mathbf{1}^T \mathbf{p} \le P_{\max} \tag{4}$$

where $\mathbf{p}$ denotes the column vector of the K powers $\{p_k\}$, $\mathbf{A}$ is a $K \times K$ matrix representing the intra-cell interference, and $\mathbf{f}$ and $\mathbf{b}$ are two column vectors of length K representing respectively the inter-cell interference and thermal noise. The quantities $\mathbf{A}$, $\mathbf{f}$, and $\mathbf{b}$ are characterized by:

$$A[k, j] = \alpha_{kj} \left(1 - \delta_{kj} \right), \quad f[k] = \frac{\beta_k}{SF} \sum_{q=2}^{Q} \frac{g_{qk}}{g_{1k}}, \quad b[k] = \frac{\beta_k}{g_{1k}} \tag{5}$$

where δ_{kj} stands for the Kronecker symbol that is equal to 1 for $k = j$ and 0 otherwise. The matrix $\mathbf{A}$ is not strictly positive since its diagonal is null, but it is regular, i.e. its square is strictly positive, and so the Perron-Frobenius theory applies [5]. It is well known from Perron-Frobenius theory for non negative matrices that the form $\mathbf{p} = \mathbf{A}\mathbf{p} + \mathbf{b}$ has a positive solution $\mathbf{p}^*$

= $(\mathbf{I}\text{-}\mathbf{A})^{-1}\mathbf{b} > \mathbf{0}$ if and only if the maximum eigenvalue of **A** is strictly less than 1. Thus, the necessary and sufficient condition to obtain a positive and finite solution in (4) is that the maximum eigenvalue μ^* of **A** is less than $1/\lambda_\phi$. This condition is generally referred to as the *pole condition*, and the maximum cell load K satisfying the pole condition is referred to as the *pole capacity* K_{pole} [4]. The positive solution $\mathbf{p}^*$ in (4) can then be determined as:

$$\mathbf{p}^* = \lambda_\phi(\mathbf{x}P_o + \mathbf{y}P_n), \quad \mathbf{x} = (\mathbf{I} - \lambda_\phi \mathbf{A})^{-1}\mathbf{f}, \quad \mathbf{y} = (\mathbf{I} - \lambda_\phi \mathbf{A})^{-1}\mathbf{b} \tag{6}$$

By taking into account the constraint of limited BS power, we define the *constrained capacity* as:

$$K_{const} = \arg\max_K \left\{ \Pr\left(\mu^* > \frac{1}{\lambda_\phi} \bigcup P_c > P_{\max} \right) \le \varepsilon \right\} \tag{7}$$

where ε denotes the maximum tolerated outage threshold typically set to 5%. The cell throughput can then be derived from (7) by multiplying K_{const} by (1-FER)R_ϕ, where R_ϕ is the single user bit rate for the physical layer configuration ϕ.

3.1 Capacity Indicator at the Link Level

Let us consider the case where $\alpha_{kj} \approx \alpha$ and $\beta_k \approx \beta$. In this case, the power $P_c = \mathbf{1}^T\mathbf{p}^*$ that is necessary to satisfy the SINR requirements can simply be written as (cf. (6)):

$$P_c = \underbrace{\frac{\lambda_\phi \beta K}{1 - \lambda_\phi (K-1)\alpha}}_{C_\phi} \underbrace{\left(\frac{1}{K} \sum_{k=1}^{K} \left(\frac{P_o}{SF} \sum_{q=2}^{Q} \frac{g_{qk}}{g_{1k}} + \frac{P_n}{g_{1k}} \right) \right)}_{T} \tag{8}$$

Note that T in (8) is independent of the physical layer configuration ϕ. Furthermore, by applying the law of large numbers, T can then be assumed independent of the cell load K. Only the factor C_ϕ remains therefore specific to the physical layer configuration ϕ and cell load K. Note that the factor C_ϕ needs only to be evaluated at the link level since it is only function of λ_ϕ, α, and β, which are outputs of the link to system level interface.

We extend the expression of the link level capacity indicator C_ϕ to the case of multiple factors $\{\alpha_{kj}\}$ as follows:

$$C_\phi = \frac{\lambda_\phi \beta K}{1 - \lambda_\phi \mu^*} \tag{9}$$

Thus, from (9), we can determine the maximum cell load K_{max} at a given C_ϕ threshold. Note that the pole capacity can simply be determined from (9) as when C_ϕ tends to infinity.

The interest of this novel capacity indicator in (9) is that it allows to evaluate at the link level the impact of the physical layer algorithms on the system capacity, i.e. without performing system level simulations. This makes it an efficient and accurate tool at the link level for optimizing the physical layer algorithms and identifying the most appropriate physical layer configurations for a given environment.

3.2 Particular Case of MMSEC Equalization

In the particular case of MMSEC equalization [7], the equalization coefficients are functions of the useful and interference powers received by the k-th user. The n-th equalization coefficient for the n-th channel coefficient $h[n]$ is obtained as:

$$w_k[n] = \frac{\sqrt{p_k g_{1k}}\,\bar{h}[n]}{\frac{P_c g_{1k}}{SF}|h[n]|^2 + \left(\frac{1}{SF}\sum_{q=2}^{Q} P_o g_{qk} + P_n\right)} \tag{10}$$

Thus, in this case, the intra-cell interference factors $\{\alpha_{kj}\}$ and inter-cell interference plus noise factors $\{\beta_k\}$, which are derived from the correlations of the equalized coefficients $\{h[n]w_k[n]\}$, become functions of the power vector $\mathbf{p}$. Thus, the power allocation problem in (4) becomes nonlinear as:

$$\mathbf{p} = \lambda_\phi(\mathbf{A}(\mathbf{p})\mathbf{p} + \mathbf{f}(\mathbf{p})P_o + \mathbf{b}(\mathbf{p})P_n) \tag{11}$$

In order to solve (11), the following recursive algorithm is used:

$$\mathbf{p}^{(r+1)} = \lambda_\phi\left(\mathbf{x}\left(\mathbf{p}^{(r)}\right)P_o + \mathbf{y}\left(\mathbf{p}^{(r)}\right)P_n\right) \quad \text{for } r = 1 \ldots N_r \tag{12}$$

where r denotes the r-th recursion. It is observed that when (11) has a solution, the recursive algorithm in (12) converges to this solution in few ($N_r \le 5$) recursions for any positive and finite initial vector $\mathbf{p}^{(1)}$.

The factors $\{\alpha_{kj}\}$ and $\{\beta_k\}$ should therefore be evaluated online for each recursion for each snapshot within the system level simulator. This highly increases the computational costs since these factors require the computation of K equalized channel coefficients correlations [6]. In order to reduce the computational costs, we make the following approximation:

$$w_k[n] \approx \sqrt{\frac{p_k}{g_{1k}}}\,v[n], \quad v[n] = \frac{\bar{h}[n]}{\frac{P_c}{SF}|h[n]|^2 + s} \tag{13}$$

where s replaces the second term in the denominator in (10) by its average value taken over the K users:

$$s = \frac{1}{K}\sum_{k=1}^{K}\left(\frac{P_o}{SF}\sum_{q=2}^{Q}\frac{g_{qk}}{g_{1k}} + \frac{P_n}{g_{1k}}\right) \tag{14}$$

Thus, by using (13) instead of (10), only one correlation, i.e. that of the equalized coefficients $\{h[n]v[n]\}$, instead of K correlations is therefore needed in order to evaluate the factors $\{\alpha_{kj}\}$ and $\{\beta_k\}$. This approximation has been validated via simulations where it is observed that using (13) instead of (10) increases the power P_c only by less than 0.25 dBw. Thus, this approximation has negligible impact on the accuracy of the capacity estimates, however, it has the major advantage of significantly reducing the time consumption at the system level simulator.

At last, it is important to point out here that since the factors $\{\alpha_{kj}\}$ and $\{\beta_k\}$ are specific to each snapshot at the system level, the capacity indicator C_ϕ, evoked in sub-section 3.1 for simple equalization schemes, becomes then specific to each snapshot. The exact value of C_ϕ cannot therefore be evaluated at the link level. However, one can still evaluate another C_ϕ at the link level by making use of the simplified link level MMSEC equalization coefficient given by [7]:

$$w[n] = \frac{\overline{h}[n]}{\frac{K}{SF}\left|h[n]\right|^2 + \sigma^2_{AWGN}} \tag{15}$$

where σ^2_{AWGN} is the variance characterizing the inter-cell interference plus noise at the link level. Thus, from (15), we can evaluate C_ϕ at the link level for different values of σ^2_{AWGN}.

4. NUMERICAL RESULTS

This section presents an illustration of the evaluation methodology presented in the previous section. It quantifies the impact of chip mapping strategies and equalization techniques on the system capacity in the context of the urban ETSI BRAN E channel model [10]. We consider six physical layer configurations resulting from the combination of either adjacent (AFM) or interleaved (IFM) frequency domain chip mapping with either EGC, MRC, or MMSEC equalization. All six configurations use the same modulation and coding scheme, which consists of QPSK-Gray modulation and UMTS-like convolutional code of rate ½. The key other parameters of the MC-CDMA physical layer are summarized in Table 1 [10].

Table 1. Key parameters of the MC-CDMA physical layer.

Sampling frequency f_s	57.6 MHz
FFT size N_{fft}	1024 samples
Guard interval size N_g	216 samples
Number of data carriers N_c	736 carriers
Frame size N_f	32 OFDM symbols
Spreading factor SF	32 chips

Table 2 summarizes the target SINR values required to achieve 1% target FER for all the six physical layer configurations. These values are obtained from [6] for a cell load K = 24. As discussed in [6], the target SINR is invariant with respect to K in the IFM context, whereas in the AFM context, it is more or less invariant for K in the range between 16 and 32. Thus, in the sequel, we confine our analysis to K between 16 and 32.

Table 2. Target SINR (dB) for 1% target FER.

	IFM context	AFM context
MRC	4.25	6.2
EGC	4.5	5.85
MMSEC	4.85	5.3

Fig. 2 illustrates the novel link level capacity indicator C_ϕ as a function of the cell load K for all the six configurations. For MMSEC equalization, we consider two values of σ^2_{AWGN} in (15): –5 dB and –10 dB. From Fig. 2, we can observe that for K between 16 and 32, AFM-EGC outperforms IFM-EGC that in turn outperforms AFM-MRC and IFM-MRC. Moreover, IFM-MMSEC and AFM-MMSEC for both values of σ^2_{AWGN} have very close performance to AFM-EGC. Thus, from this link level study, we can conclude that AFM always outperforms IFM for any given equalization technique. Moreover, AFM-EGC, AFM-MMSEC, and IFM-MMSEC are similar and provide the highest system capacity.

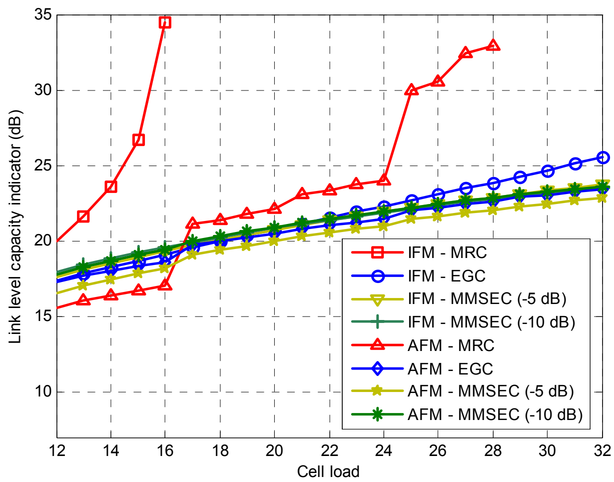

Figure 2. Link level capacity indicator (dB) versus the cell load.

Table 3 summarizes the most relevant system level parameters [10]. Note that we use the standard large-scale propagation model including path loss and log-normal shadowing [4].

Table 3. System level parameters.

Number of tiers	$N = 2$ ($Q = 19$ cells)
Cell radius	300 m
Thermal noise power density	-204 dBw/Hz
Propagation model	L = -57.45 dB, $\delta = 2.8$, σ_s = 8 dB, $\rho = 0.5$
Number of codes at BS	M = 32 codes
Outage threshold	$\varepsilon = 5$ %

Fig. 3 depicts the pole capacity and the constrained capacity for $P_{max} = 13$ dBw and $P_o = 3$ and 6 dBw. As we can see from Fig. 3, IFM-EGC, IFM-MMSEC, AFM-EGC, and AFM-MMSEC yield a full pole capacity of 32 codes. Moreover, for moderate inter-cell interference level (e.g. $P_o = 3$ dBw), IFM-MMSEC, AFM-EGC, and AFM-MMSEC yield almost the same and highest constrained capacity. However, for high and dominant inter-cell interference (e.g. $P_o = 3$ dBw), all configurations unless IFM-MRC are similar with a little advantage for AFM-EGC and AFM-MMSEC. These results match well those obtained from the previous analysis of the novel capacity indicator at the link level. Thus, for urban ETSI BRAN E channel model, AFM-EGC is the most suitable configuration since it provides the highest capacity and EGC is less complex than MMSEC equalization.

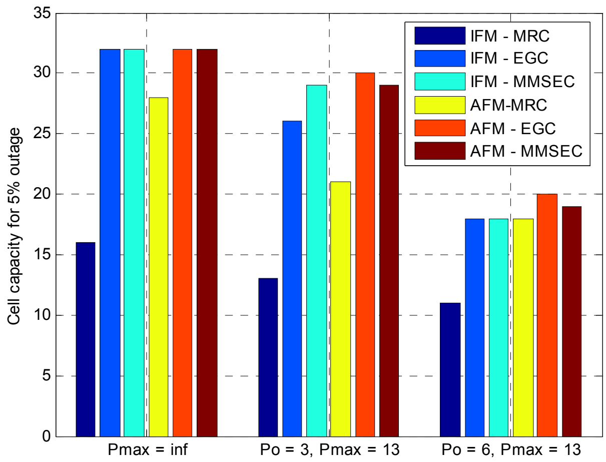

Figure 3. Pole and constrained capacity estimates.

5. CONCLUSIONS

This paper presented an evaluation methodology to quantify the impact of the MC-CDMA physical layer algorithms on the downlink capacity in a multi-cellular environment. The methodology consists of both qualitative and quantitative evaluations via link and system level analysis respectively. A very good match was shown between qualitative evaluation using a novel link level capacity indicator and quantitative evaluation using Monte Carlo statistical system level simulations. An illustration of this methodology showed that in particular adjacent frequency domain chip mapping always outperforms interleaved mapping for any given equalization technique in the context of the urban ETSI BRAN E channel model.

This methodology can further be applied to quantify the impact on the system capacity of different MC-CDMA physical layer configurations in different environments, which is crucial for system design.

6. ACKNOWLEDGMENT

The work presented in this paper was supported by the European IST project 4More (4G MC-CDMA multiple antenna system On chip for Radio Enhancements) [11].

7. REFERENCES

[1] J. Zander, S. L. Kim, "Radio Resource Management for Wireless Networks", *Artech House Publishers*, 2001.
[2] H. Holma, "A Study of UMTS Terrestrial Radio Access Performance", *Ph.D. dissertation, Helsinki University of Technology*, Oct. 2003.
[3] ETSI Technical Report 101 112, "Selection Procedures for the Choice of Radio Transmission Technologies of UMTS," *UMTS 30.03 version 3.2.0*, 1998.
[4] N. Enderlé, X. Lagrange, "Analyse de la capacité descendante d'un système WCDMA," *Actes du congrès DNAC*, Nov. 2001.
[5] E. Seneta, "Non-negative matrices and Markov chains," *Springer, 2nd edition*, 1981.
[6] A. Mourad et al., "Interface between Link and System Level Simulations for Downlink MC-CDMA Cellular Systems," *Proceedings of the 11th European Wireless Conference*, Nicosia, Apr. 2005.
[7] S. Hara, R. Prasad, "Design and Performance of Multi-carrier CDMA System in Frequency-Selective Rayleigh Fading Channels," *IEEE Transactions on Vehicular Technology*, vol. 48, no. 5, Sep. 1999.
[8] H. Atarashi et al., "Broadband Packet Wireless Access Based on VSF-OFCDM and MC/DS-CDMA," *IEEE PIMRC*, vol.3, Sep. 2002.
[9] K. Fazel, S. Kaiser, "Multi-Carrier and Spread Spectrum Systems," *John Wiley & Sons Ltd*, 2003.
[10] IST-MATRICE, *http://ist-matrice.org*.
[11] IST-4MORE, *http://ist-4more.org*.